

Figure 4.10. Twelve-hour maximum persisting 1000-mb dewpoints for October (°F).

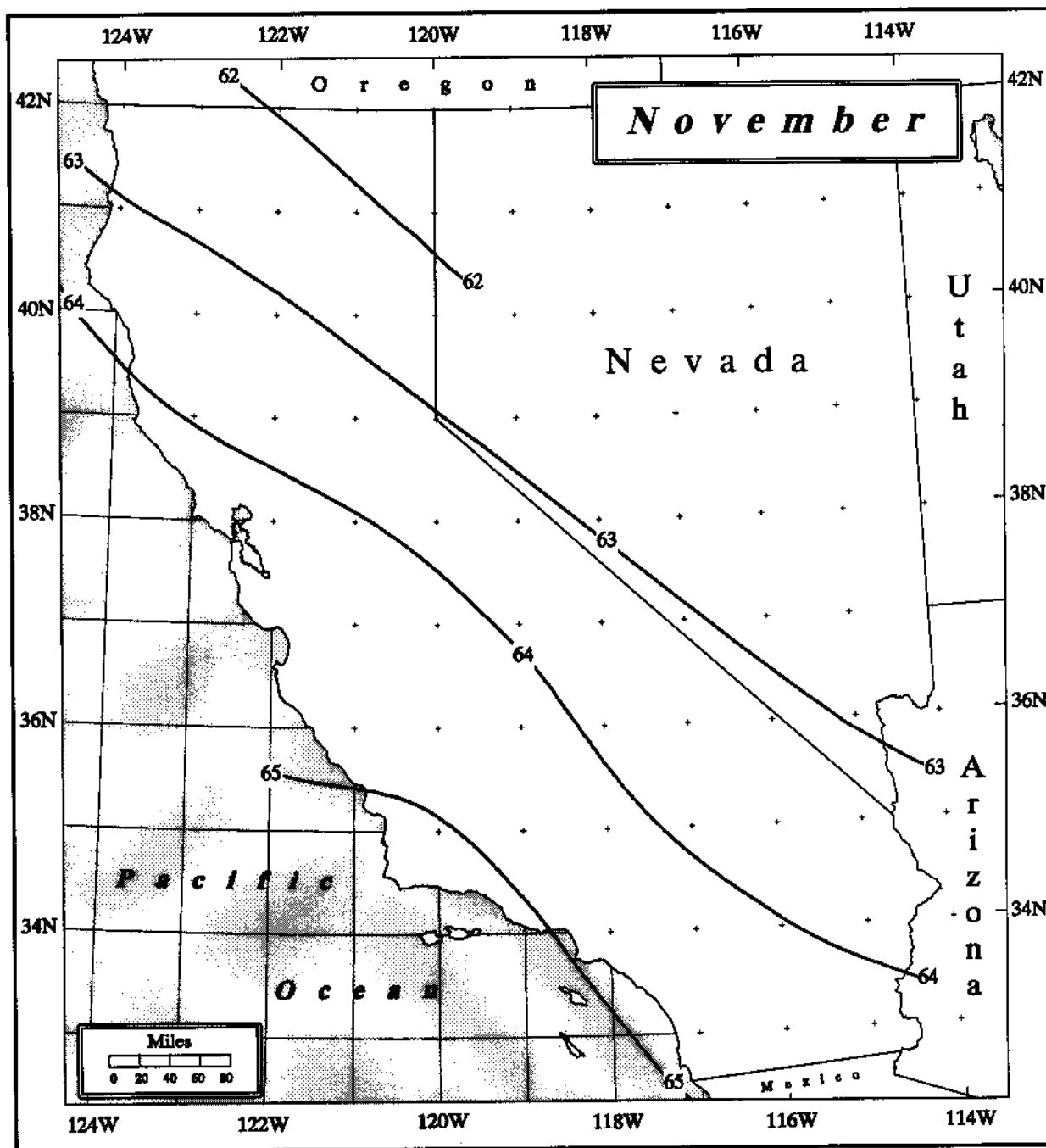


Figure 4.11. Twelve-hour maximum persisting 1000-mb dewpoints for November ($^{\circ}\text{F}$).

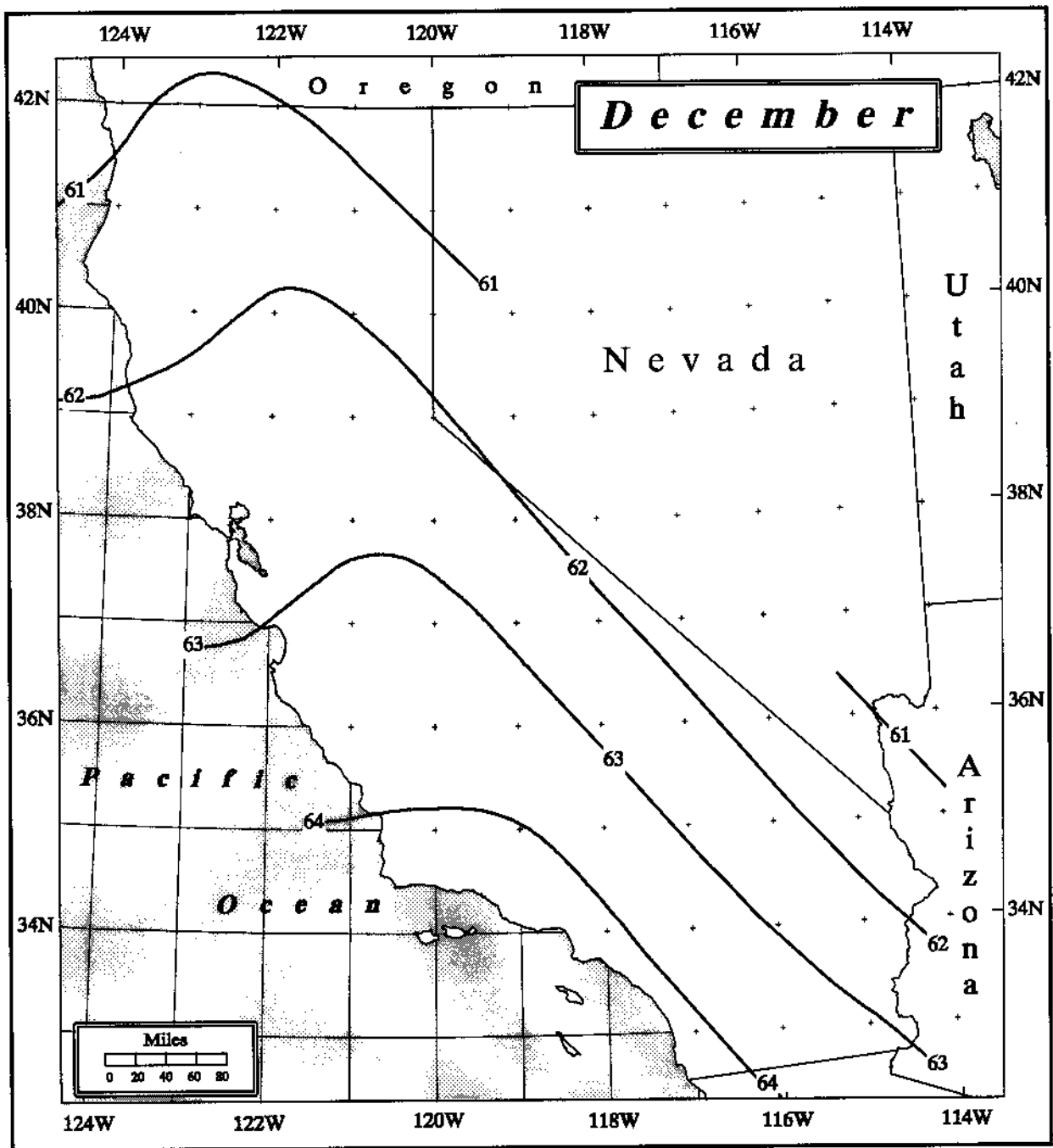


Figure 4.12. Twelve-hour maximum persisting 1000-mb dewpoints for December ($^{\circ}\text{F}$).

Four locations indicated by A, B, C, and D in Figure 4.13 were selected to monitor the monthly transition. Figure 4.14 shows the monthly variations in 1000-mb 12-hour persisting dewpoint temperatures for four locations in California. All four locations show maximum dewpoints in July to August and minimums in January or February and a smooth transition from month to month and across the year. The largest 1000-mb persisting dewpoint is over southeast California.

Figure 4.15 partitions California into three regions, each defining the months in which the largest daily precipitation amounts have been observed most frequently. The California partitions are continuous with the partitioning for Washington and Oregon shown in Figure 4.14 in HMR 57. The months with the potential of having the greatest rainstorms are: October through March in most of western California; July through October in extreme southeast California; and any month for the remainder of California. Isodrosotherms were drawn by averaging monthly dewpoint for the indicated months within the three sections. The analyses were combined by smoothing across sectional boundaries. The result was the *multi-seasonal* 12-hour maximum persisting dewpoint map shown in Figure 4.16. In the process of deriving all-season PMP values shown in Plates 1 and 2, this map was used to adjust all transposed 1000-mb free-atmospheric-forced precipitation (FAFP) values in the region to their respective barrier elevations. FAFP is convergence or non-orographic precipitation (see Chapter 6 for more explanation). The dewpoint map was also used to adjust the 100-year, non-orographic precipitation values to create the orographic parameter, T/C (Chapter 6).

Except for HMR 57, previous HMRs for the western United States have used land-based observed and maximum persisting dewpoints for storm maximization. In HMR 57, it was decided to use SST as a proxy for the *traditional* maximization factor for many storms. Many of the storms have up-wind regions with only ocean surface, and consequently no possible upwind measurements of dewpoint temperatures. For such storms SSTs were used. All these storms, had moisture trajectories originating in the Pacific Ocean. The proxy factor was based on a comparison between an observed SST and an estimated maximum SST. The maximum SST (or upper limit SST) was estimated from two standard deviations above climatology, which was at a point sufficiently upwind of the cold coastal current to be unaffected by it and along the moisture trajectory into the storm center. In HMR 57, it was

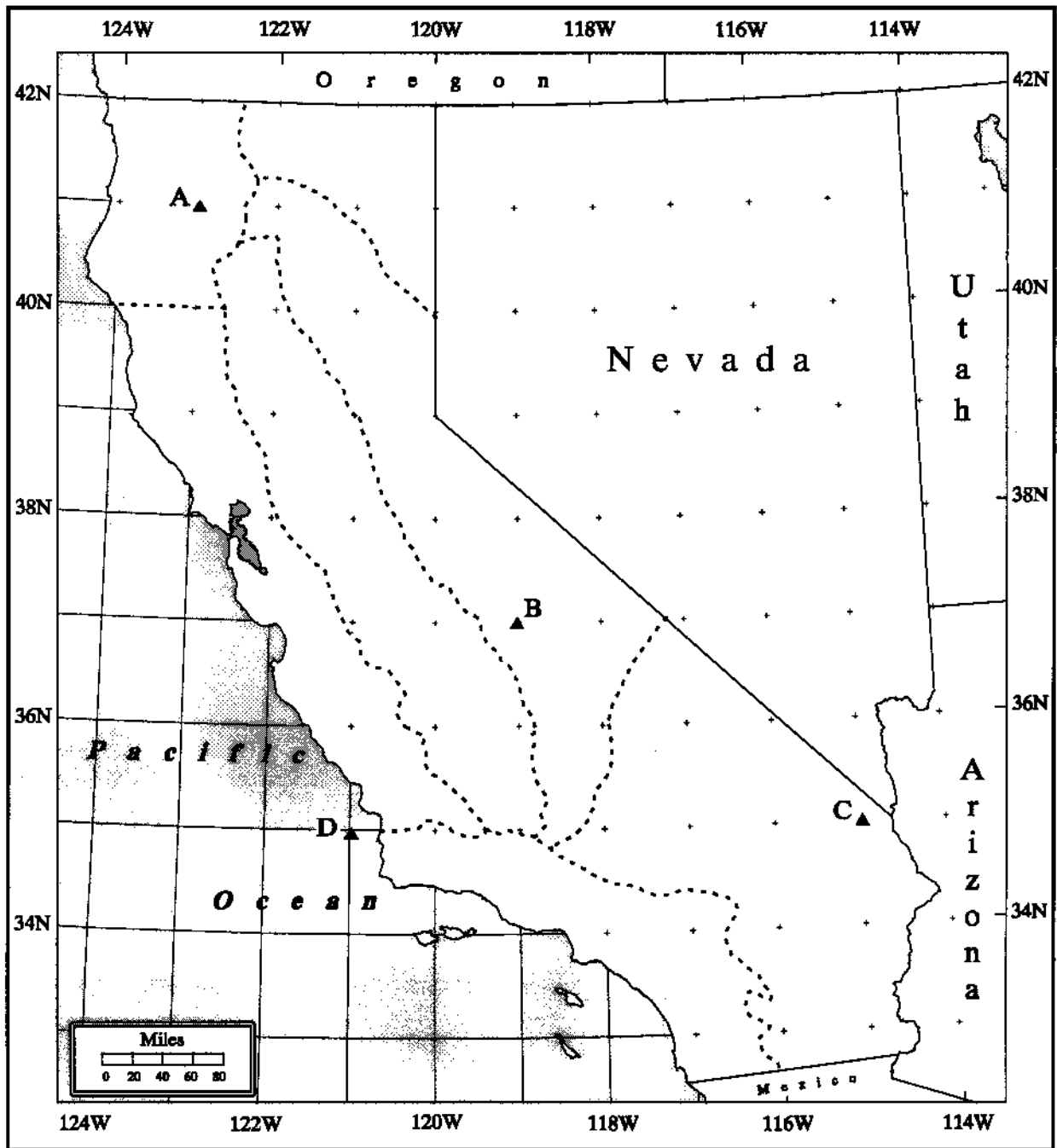


Figure 4.13. *Locations (A, B, C, D) shown for the month-to-month continuity check from January to December. Regional boundaries are shown.*

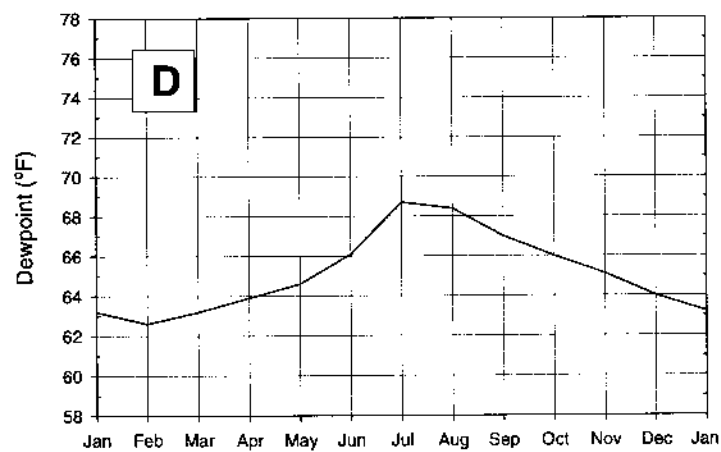
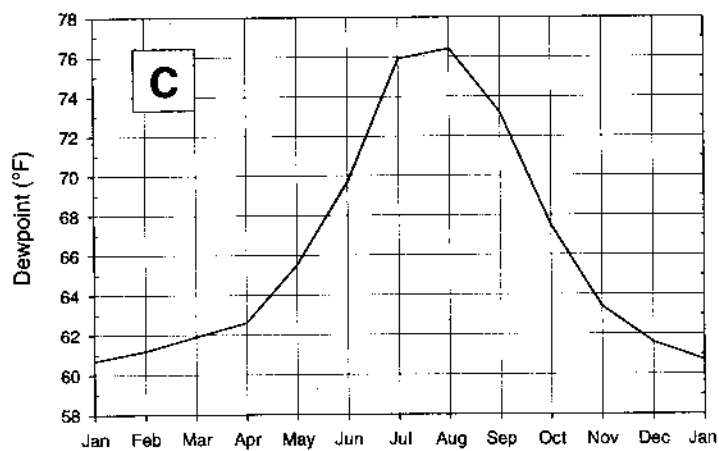
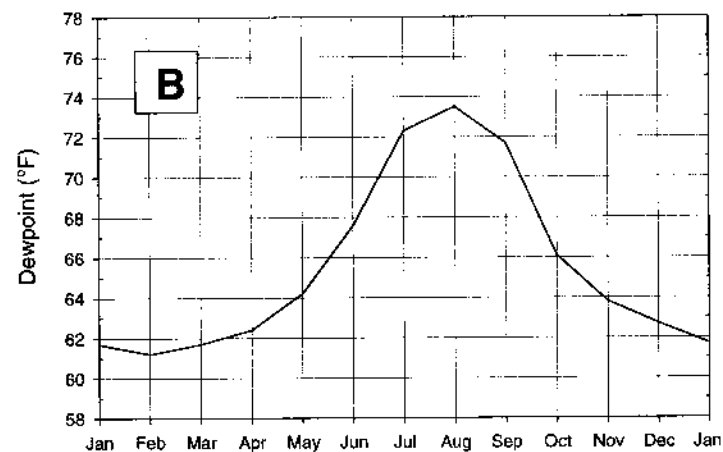
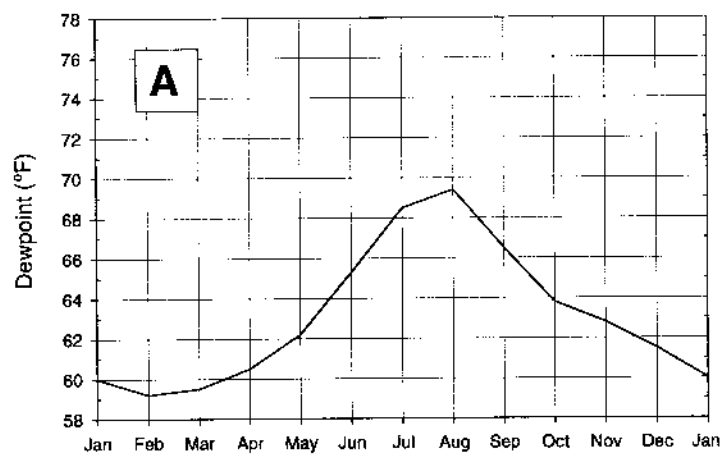


Figure 4.14. Example of consistency and smoothness checks for 12-hour maximum persisting 1000-mb dewpoint temperatures (°F) at the locations shown in Figure 4.13.

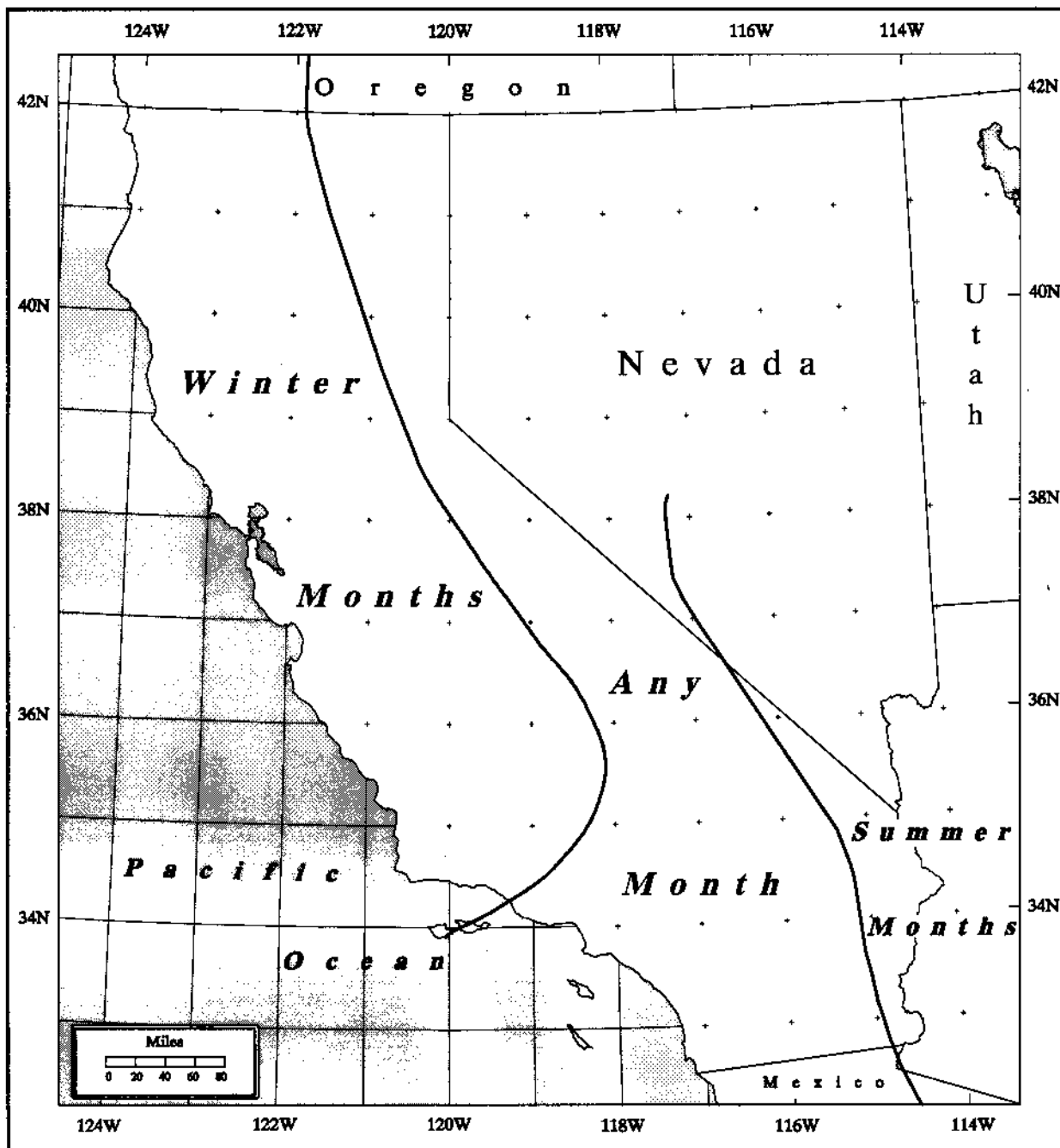


Figure 4.15. *Regions and months used in developing the multi-seasonal dewpoint maps in Figure 4.16.*

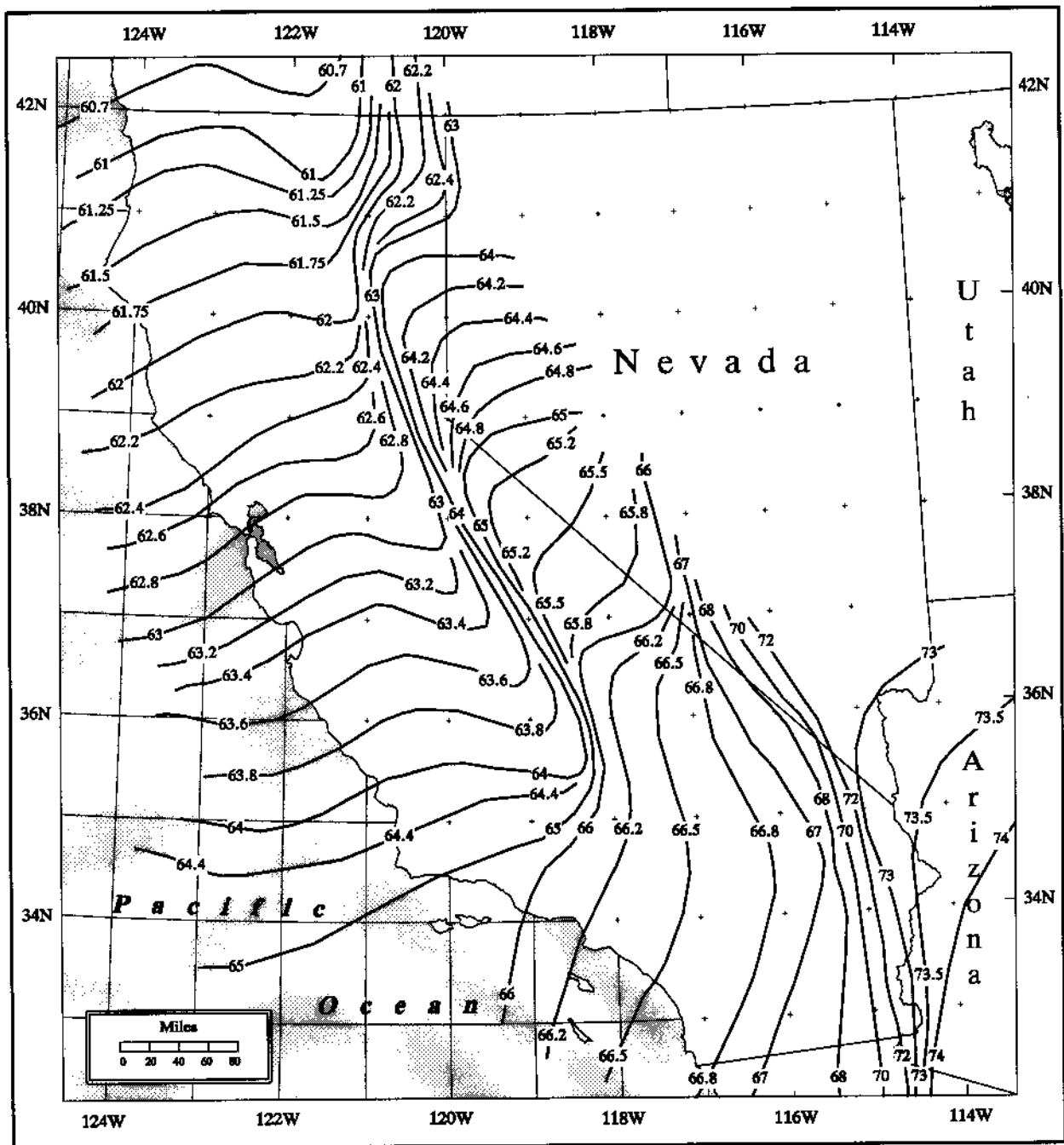


Figure 4.16. Multi-seasonal, 12-hour maximum persisting 1000-mb dewpoints used for calculating vertical adjustments (°F).

demonstrated that the proxy maximization factor remains nearly constant regardless of the amount of moisture scavenged from a parcel of air, as it crosses the cold coastal current. Therefore, it was considered reliable for setting precipitation depth for a PMP storm, as long as the assumption that the amount of scavenging in the PMP storm was the same as in an observed record-setting storm.

The Marine Climatic Atlas of the World (U.S. Navy 1981), was used to obtain the mean SSTs and standard deviations. To determine the maximum SST it was assumed that the mean SST plus two standard deviations would adequately set the upper limit for moisture *charge* or availability. The same procedures and assumptions used in HMR 57 were followed in this study. Thus, two SSTs were estimated for each storm - one for the storm being analyzed; the other, the maximum SST for the same location.

Essentially, the steps are: for the storm SST 1) a trajectory was extended upwind and backward in time from the storm center to a moisture source region in the Pacific Ocean; and then 2) a best estimate SST within the source region, based upon ship reports, was used as long as synoptic characteristics and distance from trajectory were consistent; and 3) for the maximum SST for approximately the same location, the mean SST and standard deviation were derived from the Marine Climatic Atlas for the same month, with a 15-day adjustment toward the warmest time of year (World Meteorological Organization 1986). For the September 1959 (1006) and the August 1977 (1017) storms, that do not have extended inflow trajectories, the traditional National Weather Service procedures were followed as described in the Manual for Estimation of Probable Maximum Precipitation (World Meteorological Organization 1986). Calculations of maximizing factors were made with temperatures to the nearest tenth of a degree Fahrenheit and precipitable water amounts from interpolation in precipitable water tables (U.S. Weather Bureau 1951).

All trajectories were drawn using archived surface weather maps. For storms before 1950, SST measurements came from archived ship reports from the NOAA Environmental Research Laboratory (1985), Boulder, Colorado, and the National Oceanic Data Center, Washington, DC. The analyses were supplemented by the daily weather maps (Environmental Data Services 1899-1971). The records of land station observations from the Local Climatological Data Series (NCDC 1948-) were used to obtain persisting dewpoints for traditional maximization.

Within the process of determining the appropriate SST for individual storms, some complications arose that influenced the values adopted in this study. These complications typically involved decisions about the timing of the moist air inflow. Relatively small differences in time (order of hours) could result in widely different source regions (order of degrees of latitude/longitude). Additional analysis was used to resolve any inconsistencies.

5. STORM ANALYSIS

5.1 Introduction

A complete analysis of 31 storms listed in Chapter 2, Table 2.1 was done to produce depth-area-duration (DAD) relations. Although the procedure is similar to past storm studies and hydrometeorological reports, no previous DAD relations were accepted for this study, except from storms used in HMR 57 (1994); otherwise, uniformity of analysis could not be assured. Each storm was individually examined and analyzed based upon all available data. Although previous storm DADs were available from the Corps of Engineers Storm Rainfall Catalog and from unofficial DAD studies completed by the National Weather Service (NWS), new DADs were developed. Previous storm analysis procedures were labor-intensive and time-consuming. However, with the help of a geographic information system (GIS) the storm studies were completed more expeditiously and efficiently.

As a result of using a more automated approach to calculate DAD for the storms, less time was spent in routine procedures and manual drawing of various maps. The use of a GIS system (GRASS 4.0 1991) and computer spreadsheets minimized many of the computational aspects. For instance, data tabulation for specific storm periods, mass curves for each station (hourly and daily), DAD analysis, and pertinent data sheet preparation were all done by computer. However, much time was still needed for quality control, formatting, and entering supplemental data (data not part of the regular NWS network of stations, such as bucket survey data).

As in HMR 57, the spatial distribution of storm rainfall was determined by comparing the proportion of storm rainfall to the 100-year frequency analyses in NOAA Atlas 2 (1973). The 100-year precipitation analysis shows considerable correlation with the underlying terrain, and the choice was made for this very reason. But it is also understood that individual storm precipitation could have different spatial distributions than shown in the atlas.

5.2 Precipitation Data

Precipitation data come from various sources and are the foundation for all storm DAD results and eventually PMP estimates. A thorough search was made for all recorder (hourly), non-recorder (daily), and supplemental (bucket survey and partial record stations) data available for all storms on the storm list (Chapter 2, Table 2.1). The majority of the data came from official NWS sites, both first order and cooperative stations. Supplemental data are data not normally archived by the NWS. For example, bucket surveys may be conducted by local, state, or federal officials. Such surveys provide invaluable data sets for a storm, especially in areas of limited information. The post-1948 NWS data were in digital form and converted to a standard internal format. The supplemental data and observation times for each observation were entered manually. Occasionally observation times, especially for older storms, were not extremely precise. For example, some observation times are given as sunrise or sunset, or as morning or evening with no set time indicated. Timing for these observations were determined by checking with nearby stations. The observation-entering stage was also the beginning of the quality-control as every station was examined for anomalous and incorrect information. Problems with accumulated amounts (precipitation for a multi-day storm period totaled into one observation usually at the end of the storm), missing data, and incorrect or ambiguous observation times, were addressed. Missing observations during the storm period usually caused the station to be discarded. Accumulated precipitation amounts for the storm period were useable if the observation began and ended within the storm period.

Once all of the quality-controlled data were put into a common format, each daily and supplemental station was timed. Timing provides a consistent temporal and spatial precipitation distribution for all stations within a storm. Thus, instead of just a few stations with hourly records, now all stations have an hourly distribution. A station was timed by assigning each daily station to an hourly station in order to distribute the daily station's rainfall in the same manner as the hourly station. The hourly station controls the hour when the rainfall began, the intensity of rainfall during the rain event, and when the rainfall ended at each of the daily stations assigned to it. In other words, the hourly station defines how the daily precipitation fell during the storm period at the daily stations.

Criteria for timing the stations included: distance between the hourly and daily

stations, topography, and the precipitation observed at the hourly and daily stations assigned to each other. Topographical considerations included the closeness of stations, valley/slope relations, and the location of crestlines. After all daily stations were assigned to an hourly station, daily precipitation was distributed into hourly increments across the storm period. Using the hourly distribution of rainfall, the observation times, and the amounts at the daily stations, the rainfall at the daily and supplemental stations was allocated according to the hourly station distribution. This process was done iteratively so that if an hourly distribution failed to provide adequate or realistic results, another nearby hourly station could be used instead. The distributions were compared by graphing the results, using mass curves, and examining them for consistency.

Figure 5.1 shows an example of one of the mass curves, for the January 20-24, 1943 storm (1003), and illustrates the consistency between the daily and hourly stations. Hoegees Camp was the hourly station used to time the other stations. For this set of stations, little or no rain was observed in the first 24 hours of the storm period. The rains began at hour 26 and continued to accumulate through hour 78. A total 37.34 inches was observed at Hoegees Camp and Camp Leroy Hoegees. These 2 stations are less than a mile apart. Lesser rainfall amounts were observed at the other stations. Daily total amounts were used for each of the other stations, and the daily totals were timed individually for each day. Most general storms exhibit a fairly uniform temporal distribution.

5.3 Storm Depth-Area-Duration Analysis Procedure

The first step in defining the development of DAD relations requires that rainfall amounts be assigned to all areas in the storm. In the past, point precipitation amounts were interpolated by assigning a particular precipitation gauge to a region. Usually the rain gage was centered in the domain. Once the entire storm area was assigned to particular gages, the rainfall distribution of those gages was used to determine the precipitation sequence for each individual region (Thiessen 1911). The Thiessen technique works well in non-orographic terrain. However, in mountainous areas, such as California, a modified approach was used to describe or develop likely rainfall patterns that fell over varying topographic features. The technique used here is similar to that in HMR 57. In order to construct a model for California and distribute rainfall over areas lacking in observations, a detailed map of the percent of total storm precipitation to the 100-year, 24-hour precipitation frequency (NOAA

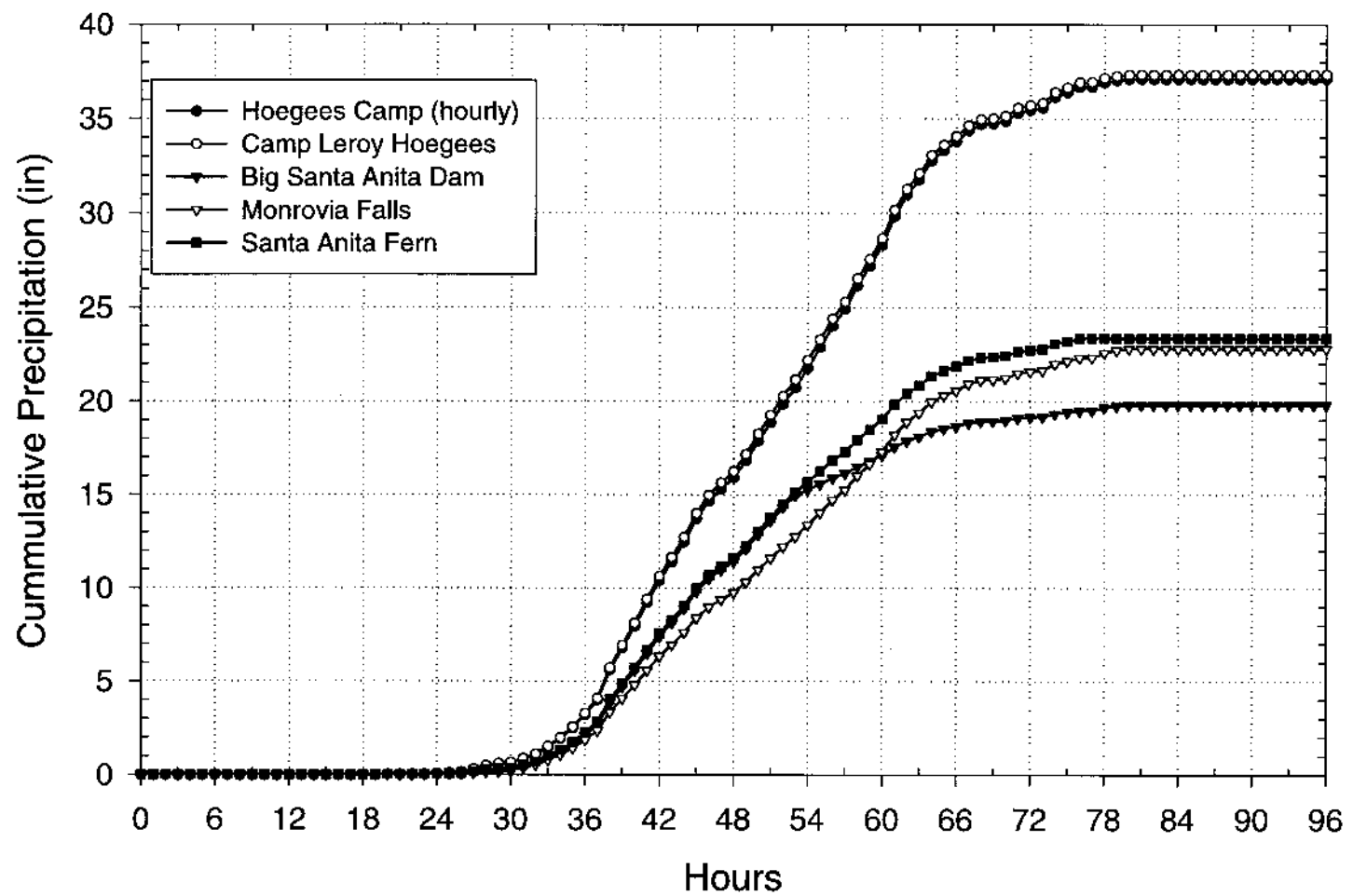


Figure 5.1. *Mass curves for four daily stations using Hoegees Camp as the hourly recorder for the January 20-24, 1943 storm (1003).*

Atlas 2) was produced. This map, called an isopercental map, represents the percentage of total storm rainfall to the 100-year, 24-hour analysis. Figure 5.2 shows a portion of an isopercental map from the January 20-24, 1943 storm (1003). The map was digitized using a GIS, and then interpolated, resulting in a raster field of percentals for the storm region. The process consisted of digitizing isolines which are considered vectors in a GIS. Vectors are the computer interpretation of an isoline. An interpolation between vectors forms a continuous field of values called a raster field in which each point (or raster) on the map has a value. Each raster cell was a 15 second by 15 second region (about 0.08 mi²) and had a interpolated value related to it. Next, the rainfall over the whole area is distributed temporally. Individual subareas of the total storm pattern are delineated, with a representative individual station mass curve. Representative subareas or polygons were drawn by first choosing the station that best represented the total precipitation and rainfall distribution for the area. Then, a border was drawn that encompasses that region which is meteorologically and topographically homogeneous. A portion of the polygon map for the January 20-24, 1943 storm (1003), is shown in Figure 5.3. The polygons were drawn with the synoptic situation, terrain, and station type (hourly, daily, or supplemental) taken into consideration. There is no uniform rule as to the number of sides or the size of the polygon as long as the station chosen represents the precipitation distribution for that area. Drawing to terrain features often produces polygons that are not like those in a classic Thiessen polygon analysis since those Thiessen polygons do not follow the terrain features.

With the completion of the polygons, total storm precipitation values and their appropriate hourly distribution were determined using a GIS. A total storm precipitation map for the area was created by multiplying the isopercental raster layer by the 100-year, 24-hour precipitation frequency raster layer from NOAA Atlas 2. The temporal distribution of precipitation at each point within the storm area was then calculated by combining the polygon raster layer, containing the temporal distribution of the previously assigned station, and the total precipitation raster layer. Once the temporal distribution field was defined, total storm precipitation was distributed into a field of hourly values for the storm. All computations were done using GRASS 4.0 (1991) GIS at 15-second intervals (0.08 mi²).

An isohyetal map was made for total storm rainfall for each storm, based on the total storm precipitation layer. Figure 5.4 shows a portion of the isohyetal map for the January 20-24, 1943 storm (1003). The isohyetal map identifies regions of peak precipitation. It is

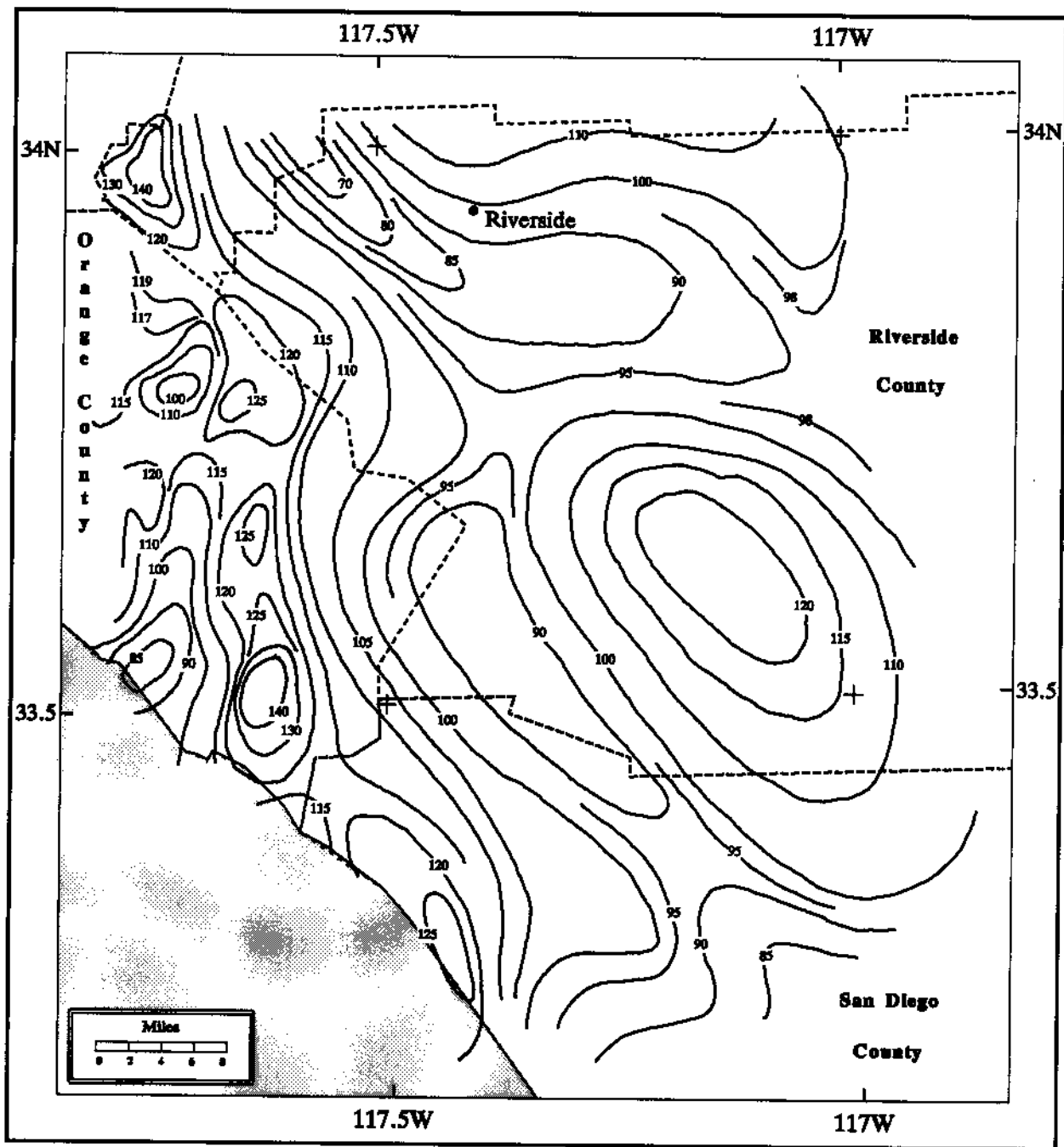


Figure 5.2. *An example of isopercental lines drawn for the January 20-24, 1943 storm (1003). The values represent the percent of the total storm rainfall to the 100-year, 24-hour precipitation frequency (NOAA Atlas 2, 1973).*

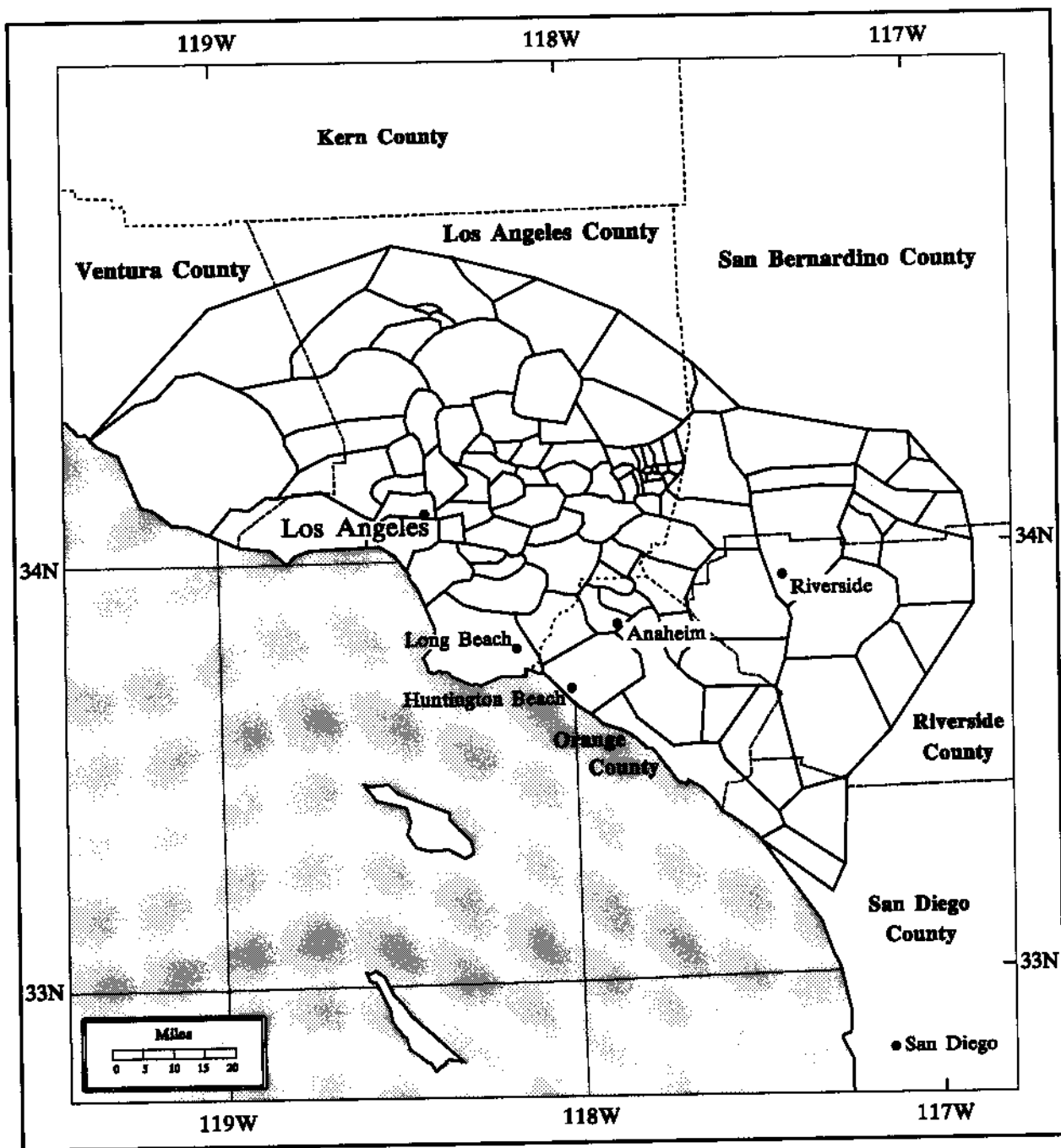


Figure 5.3. *An example of a polygon map used for analysis in the January 20-24, 1943 storm (1003).*

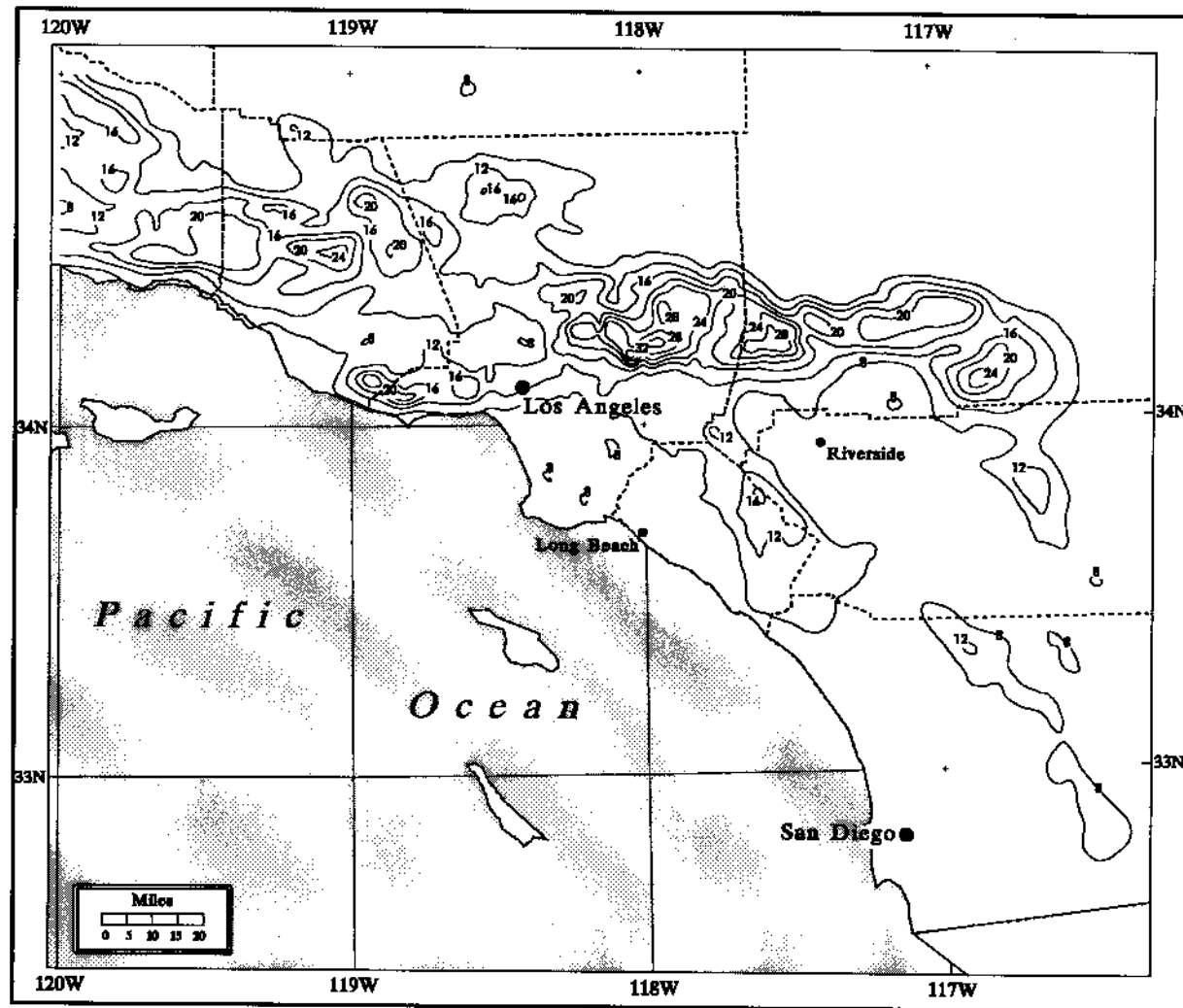


Figure 5.4. *Precipitation for the January 20-24, 1943 storm (1003). Isolines begin at 8 inches with 4-inch intervals up to 32 inches.*

important to identify the maximum precipitation center(s) for determining the DAD for a storm. Often in complex terrain, several significant precipitation peaks occur. Since combining precipitation centers miles apart is akin to combining nonhomogeneous meteorological factors and/or moisture supply, only those centers that were judged to be from the same dynamic mechanisms and moisture supply were combined. To choose which precipitation center would provide the maximum depth at a given area size and for a particular duration, several centers were examined separately. Precipitation centers occurring near one another were consolidated if the same convergence/orographic mechanisms appeared responsible for the precipitation. Multi-center storms normally occur along mountain chains where nearby peaks become precipitation centers. A common example of a split center is one center along the Coastal range and a secondary maximum over the Sierra Nevada mountains. The Coastal range center(s) almost certainly had differing orographic and convergence components than the Sierra center and therefore differing dynamic mechanisms. Split centers of this type occurred in more than half of the storms examined.

Storm DAD was calculated with a program developed with a C-language interface provided with GRASS 4.0. The output from the DAD program was plotted and examined on semi-log paper with the precipitation depth on the x-axis and the area on the y-axis. A graph was made for each duration interval (1, 6, 12, 24, 36, 48, 60, and 72 hours). The values on the graph reflect the greatest precipitation depth for various area sizes and for various durations of the storm based upon a particular storm center. The maximum depth for various area sizes was determined for each duration. Care was taken to insure spatial and temporal consistency with the storm center. A line was drawn to connect those points with the same center from 1 mi² to beyond 10,000 mi² at the upper areal limit.

Finally, after the DAD lines connecting all of the maximum precipitation amounts were drawn for the storm, precipitation values were extracted for selected durations and area sizes and placed on a pertinent data sheet. Table 5.1 presents the results for the January 20-24, 1943 storm (1003). This pertinent data sheet was the culmination of the entire storm analysis procedure.

Table 5.1. *Precipitation from the January 20-24, 1943 storm (1003) by area and duration (inches.)*

Area (mi ²)	Duration (hours)											
	1	3	6	12	18	24	36	48	60	72	84	96
1	2.90	5.50	9.50	16.05	20.52	25.70	33.18	36.10	36.51	36.52	36.54	36.65
10	2.43	4.78	8.55	14.62	17.80	22.90	28.76	31.60	32.28	32.30	32.86	33.00
50	2.14	4.25	7.85	13.15	16.38	20.62	26.32	28.82	29.91	30.63	30.81	30.95
100	1.97	3.92	7.25	11.77	15.42	19.60	24.96	27.63	28.56	29.19	29.25	29.38
200	1.80	3.57	6.63	10.80	14.70	18.38	23.41	26.18	26.91	27.11	27.23	27.31
500	1.65	3.20	5.91	10.28	13.38	16.62	21.13	23.55	24.16	24.52	24.62	24.65
1000	1.30	2.78	5.02	8.60	11.25	14.25	18.45	20.51	21.27	21.54	21.55	21.56
2000	0.97	2.04	4.59	7.55	9.70	12.00	16.02	17.33	18.69	18.79	18.83	18.84
5000	0.62	1.80	3.50	5.78	7.50	9.50	13.32	14.79	15.60	15.78	15.86	15.88
10000			2.67	4.38	5.75	7.25	10.21	11.45	12.01	12.40	12.78	12.80
20000				3.00	4.17	4.92	7.14	7.90	8.77	9.05	9.28	9.45
30000					3.00	3.20	5.36	6.30	6.78	7.20	7.32	7.40

The final numbers were normalized and compared with other storms in the same region to create DAD curves for each region. To normalize the pertinent data sheet values for each storm, each depth at each duration was divided by the 10-mi² value at that duration. Table 5.2 contains the normalized values for the January 20-24, 1943 storm (1003).

Table 5.2. *Ratio of DAD rainfall to the 10-mi² DAD rainfall for the January 20-24, 1943 storm (1003).*

Duration (hours)												
Area (mi ²)	1	3	6	12	18	24	36	48	60	72	84	96
1	119	115	111	110	115	112	115	114	113	113	111	111
10	100	100	100	100	100	100	100	100	100	100	100	100
50	88	89	92	90	92	90	92	91	93	95	94	94
100	81	82	85	81	87	86	87	87	88	90	89	89
200	74	75	78	74	83	80	81	83	83	84	83	83
500	68	67	69	70	75	73	73	75	75	76	75	75
1000	53	58	59	59	63	62	64	65	66	67	66	65
2000	40	43	54	52	54	52	56	55	58	58	57	57
5000	26	38	41	40	42	41	46	47	48	49	48	48
10000			31	30	32	32	36	36	37	38	39	39
20000				21	23	21	25	25	27	28	28	29
30000					17	14	19	20	21	22	22	22

5.4 Storm Separation Analysis

The Storm Separation Method (SSM) is used in hydrometeorological analysis to arrive at an approximation of the non-orographic component of precipitation from storms centered in orographic areas. The SSM was originally developed for HMR 55A (1988) as a standardized procedure to isolate and quantify orographic from non-orographic factors in record-setting storms. The SSM incorporates both the moisture-maximizing process and the adjustment of dewpoints to a common reference level of 1000 mb as described in Chapter 4. The technique is fully described in Chapter 7 of HMR 55A and in Chapter 6 and Appendix 3 of HMR 57. The values produced by the SSM provide the starting point for making an index map of non-orographic PMP or free-atmospheric-forced precipitation (FAFP) to be discussed in Chapter 6. The FAFP index map, when modified by orographic factors, becomes the first approximation to the PMP Index map discussed in Chapter 7.

The SSM was performed on all storms listed in Chapter 2, Table 2.1. However, only 19 of those storms plus two Arizona storms (September 1939 (3) and September 1980 (8)) proved to have large enough index values of FAFP to warrant their transposition. Of the 21 storms of Table 5.3 only nine provided controlling values across California. The areas controlled by these nine storms are found in the next chapter in Figure 6.2. The controlling storms are noted by asterisks in Table 5.3.

Table 5.3 contains a variety of information for the 21 most significant storms. The FAFP point values from these storms were used to develop an areal analysis of FAFP for California which in turn is a component of the final PMP index values for the state.

It may be of interest to note that, the FAFP (adjusted to 1000 mb) for the December 1921 (40), November 1961 (149), and August 1977 (1017) storms was larger than the observed amount. Causitive factors for these high FAFP values include: the observed highly non-orographic precipitation at storm centers, and the substantial effects of both the moisture maximization and the vertical adjustment factors.

Table 5.3. Storms studied using the storm separation method (SSM). The 9 controlling storms are indicated by *.

Storm ID #	Storm Dates	Storm Center (decimal degrees)	10-mi ² , 24-hour precip. (inches)	1000-mb, 10-mi ² , 24-hour FAFP (inches)
508	1/15-19/1906	39.9 / 121.6	14.8	6.7
525	1/1-4/1916	39.8 / 121.6	10.1	7.6
544	12/9-12/1937	40.2 / 121.4	15.3	10.8
572	12/21-24/1955	38.0 / 119.3	13.4	7.2
575	10/11-13/1962	40.0 / 121.5	19.7	7.6
* 630	1/3-5/1982	37.1 / 122.0	20.7	10.8
1002	2/27-3/3/1938	34.2 / 117.5	20.3	7.1
* 1003	1/20-24/1943	34.2 / 118.0	22.9	9.1
* 1004	11/17-21/1950	39.2 / 120.5	12.0	9.8
1005	1/25-27/1956	34.2 / 117.5	11.5	8.1
1006	9/17-20/1959	40.7 / 122.3	17.8	7.8
1007	12/4-6/1966	36.3 / 118.6	21.7	4.3
1008	1/23-26/1969	34.2 / 117.6	19.1	4.1
* 1010	2/14-19/1986	39.9 / 121.2	18.1	11.7
* 1017	8/15-17/1977	34.8 / 115.7	5.7	9.1
Other Storms				
* 40	12/9-12/1921	48.0 / 121.4	8.1	8.7
* 88	12/26-30/1937	44.9 / 123.6	10.8	7.6
* 149	11/21-24/1961	42.2 / 123.9	10.9	12.7
* 165	1/14-17/1974	41.1 / 122.3	10.3	7.6
3	9/3-7/1939	34.7 / 113.2	4.6	1.9
8	9/4-7/1970	33.8 / 110.9	10.6	3.5

6. CONVERGENCE AND OROGRAPHIC COMPONENTS OF PMP

6.1 Introduction

The rationale for estimating a convergence or non-orographic component of precipitation in record-setting storms in regions of significant topography is that precipitation in extreme storms there is so tied to topographic variation that re-creation of the same set of record-storm conditions is unlikely anywhere else. The Storm Separation Method (SSM) addresses this theory by extracting the influence of topography from the observed precipitation, thereby permitting more extensive transposition of the storm *mechanism* responsible for the remaining non-orographic precipitation. Thus, the creation of a non-orographic probable maximum precipitation (PMP) map within extensive orographic areas is made possible.

6.2 Moisture Maximization

Both the traditional approach to moisture maximization using dewpoint observations from coastal or inland locations (WMO Operational Hydrology Report No. 1 (1986), Chapter 2, and HMR 51 (1994), Chapter 2) and maximization based on a climatology of sea surface temperatures (SST) upflow of storms (HMR 57 (1994), Chapter 4) were employed in this study. Table 6.1 shows the moisture maximization factors for the SSM analyses for 21 storms. Dewpoints with an asterisk are land-based, maximum 12-hour persisting dewpoints adjusted to 1000-mb; all others are mean SSTs plus two standard deviations from the Marine Climatic Atlas of the World (U.S. Navy 1981). Although some of the same storms were used in HMR 57, there were slight differences in method. In HMR 57 the December 1921 (40), November 1961 (149), and January 1974 (165) storms were analyzed using land-based extreme dewpoints at the storm center; for HMR 59, the SSTs were taken at a reference location upflow of the cold Pacific coastal current. The moisture maximization factor is calculated from the following expression:

Table 6.1. *In-place maximization factors from storms used to prepare the free-atmospheric forced-precipitation map. Asterisks indicate land-based dewpoints; all others are sea surface temperatures (SST).*

Storm ID	Date	Maximization factor	Barrier Elevation (ft)	Observed Temp. (°F)	Upper Limit Temp. (°F)	Land-Based Reference Location
Storms						
508	1/15-19/1906	1.24	2600	70	74	
525	1/1-4/1916	1.39	2000	69	76	
544	12/9-12/1937	1.39	5500	66	72	
572	12/21-24/1955	1.58	10,500	72	78	
575	10/11-13/1962	1.19	5500	72	75	
630	1/3-5/1982	1.35	950	66	72	
1002	2/27-3/3/1938	1.48	4400	70	77	
1003	1/20-24/1943	1.37	2100	69	75	
1004	11/17-21/1950	1.29	6900	71	75	
1005	1/25-27/1956	1.22	3900	66	70	
1006	9/17-20/1959	1.50	1000	*38	*69	Red Bluff, CA
1007	12/4-6/1966	1.39	8000	70	75	
1008	1/23-26/1969	1.33	5500	72	77	
1010	2/14-19/1986	1.26	5200	66	70	
1017	8/15-17/1977	1.39	3750	*73	*79	Phoenix, AZ
Storms used in other HMR studies						
40	12/9-12/1921	1.42	500	64	71	
88	12/26-30/1937	1.54	1500	*60	*68	Valsetz, OR
149	11/21-24/1961	1.47	2700	60	67	
165	1/14-17/1974	1.23	3300	66	70	
3	9/3-7/1939	1.30	2200	*72	*77	Gila Bend 30 SW, AZ
8	9/4-7/1970	1.32	4400	*73	*78	Phoenix 55 SW, AZ

$$R_{lp} = \frac{W_{p, SL, SE}}{W_{ps, SL, SE}} \quad (6-1)$$

where,

R_{lp}	=	In-place maximization factor
W_p	=	precipitable water associated with 12-hour maximum persisting dewpoint
W_{ps}	=	precipitable water associated with 12-hour persisting dewpoint for storm 's'
SL	=	storm location
SE	=	storm barrier elevation

6.3 Horizontal and Vertical Adjustment Factors

Horizontal transpositions were done on a 1000-mb surface, and therefore, the SSM-derived, in-place maximized, non-orographic moisture was adjusted to 1000 mb. The adjustment factor is based on the difference in moisture available for precipitation between the storm's barrier elevation and 1000-mb, in a saturated pseudoadiabatic atmosphere (U.S. Weather Bureau 1951). No changes were made in the first 1000 feet of vertical transposition. All vertical adjustments were *downward* and were, therefore, equal to or greater than 100 percent. The adjustment is calculated from the following expression:

$$R_{vt} = \frac{W_{p \max, SL, SE, 1000 \text{ mb}}}{W_{p \max, SL, SE \pm 1000 \text{ feet}}} \quad (6-2)$$

where,

R_{vt}	=	vertical adjustment factor
$W_{p \max}$	=	precipitable water associated with 12-hour maximum persisting dewpoint
SL	=	storm location
SE	=	storm barrier elevation
1000 mb	=	sea-level equivalent height
$SE \pm 1000$	=	1000-foot exclusion from adjustment

Figure 6.1 is a graphical representation of this expression for selected dewpoints.

The maximized, non-orographic record-setting storm amounts were adjusted from their elevations of occurrence to a common surface at 1000 mb. Next they were transposed along the 1000-mb surface within certain meteorological and orographic constraints, more fully described in Section 6.3. When a storm is transposed it is assumed that the same meteorological dynamics can be assembled in another location. The only difference between the vertically-adjusted and maximized observed precipitation amount at its origin, and the precipitation amount at the transposed location is from differences in moisture availability between the two locations, i.e., the differences would be based on the climatology of moisture for the region involved.. The gradients of maximum 12-hour persisting dewpoints at 1000 mb are the basis for the horizontal adjustments. Figures 4.1 to 4.12 (Chapter 4) show the fields of dewpoints involved in this adjustment. The adjustment is calculated from the following expression:

$$R_{HT} = \frac{W_{p \text{ max, TL, 1000 mb}}}{W_{p \text{ max, SL, 1000 mb}}} \quad (6-3)$$

where,

R_{HT}	=	horizontal transposition adjustment factor
$W_{p \text{ max}}$	=	precipitable water associated with 12-hour maximum persisting dewpoint
TL	=	transposed location
SL	=	storm location

The date of the storm determines which monthly dewpoint chart is to be used.

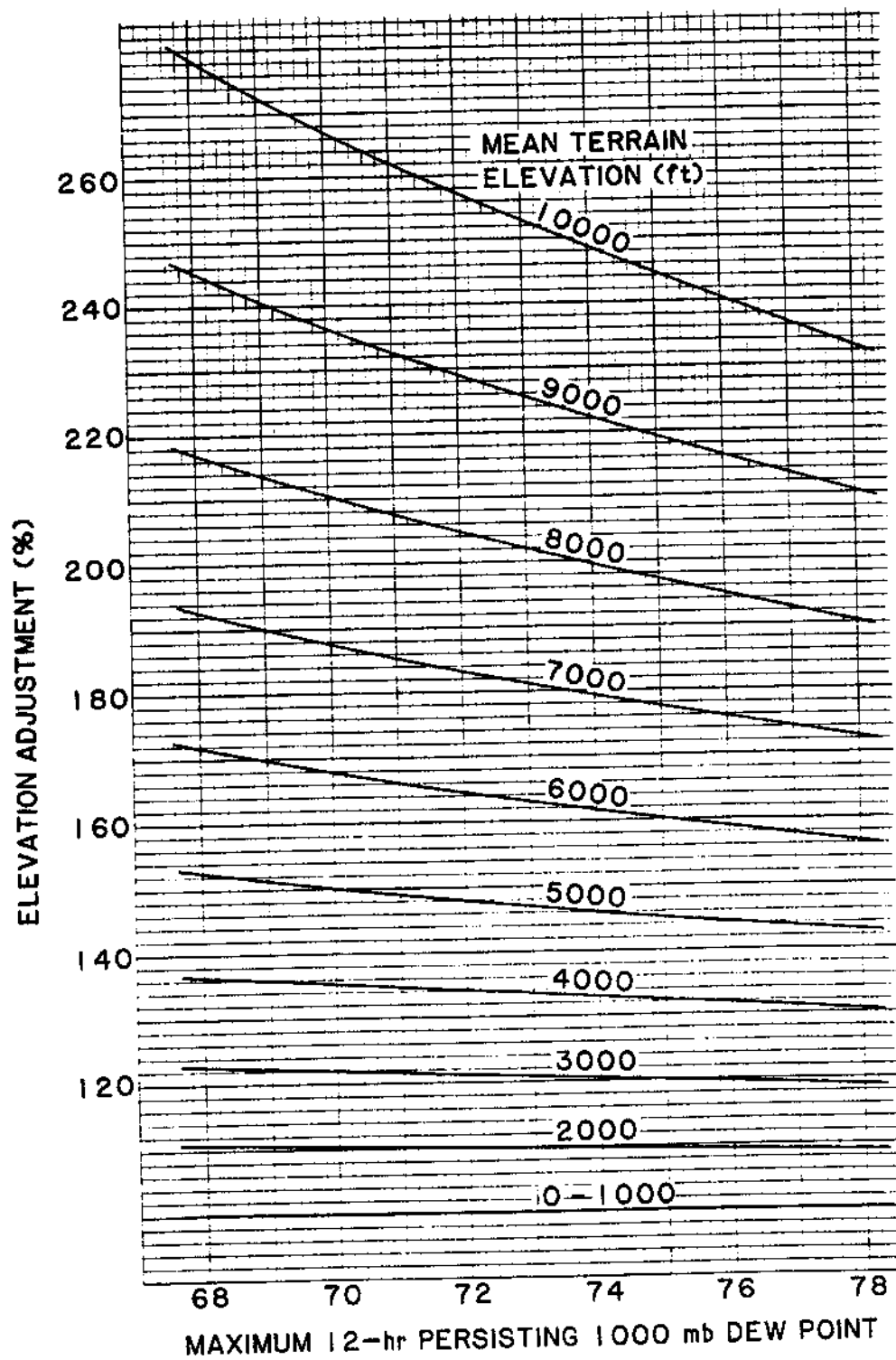


Figure 6.1. *Factors (%) for vertical adjustment of storm amounts at selected barrier elevations and dewpoint temperatures.*

6.4 Vertical and Horizontal Range of Transposition

Storm transposition involves relocating the atmospheric features of a storm from the place where they occurred to places where these features could be reassembled in the same way. It is not the storm precipitation as such which is transposed, rather it is the thermal and dynamic properties of the atmosphere responsible for the precipitation that are transposed.

The first step used to set the horizontal limits of transposition was a meteorological classification of each storm. Storm classification system was based on the factors most important for occurrence of extreme rainfall and is the same as the system developed for HMR 55A. In California the classification contains two major groups, general cyclonic and convective. The convective group is divided into complex and simple systems; cyclonic storms are divided into tropical and extratropical. And finally, extratropical storms are divided into frontal and convergence events (HMR 55A (1988), Chapter 2 and HMR 57, Chapter 7). Table 6.1 shows 21 storms that were classified, 19 as cyclonic and 2 as convective. The cyclonic storms were extratropical except for the September 3-7, 1939 storm (3). The principal forcing factor in 7 of the 19 storms was the circulation and associated convergence/divergence fields, whereas thermal contrasts and frontal displacements were paramount in the other 12 storms. Cyclonic storms were found in all regions of California, except the Northeast. It was determined that the November 1950 storm (1004) was transposable to the Northeast since it was north of the 39th parallel, and occurred at a significantly more remote site than other Sierra storms. The January 1974 storm (165), originally analyzed for HMR 57, occurred near the border between the Northeast and Sierra regions and was also considered transposable to the Northeast. Thus, at the first stage of transposition, all of California was covered by storm mechanisms classified as cyclonic.

The September 1959 (1006) and August 1977 (1017) storms were convectively driven. Although they were found in the extreme northern Central Valley and in the Southeast region, respectively, it is believed that such storms could occur anywhere in California. However, it was judged that only in the Southeast and in the northern Central Valley could convection develop well enough to become the mechanism responsible for non-orographic PMP at 10-mi² and 24-hours, regardless of season. Hence, at the first approximation of transposition limits, these two storms were confined to their region of

occurrence. Even though the September 1959 storm (1006) was estimated to have produced the largest non-orographic amount of precipitation in the northern Central Valley among storms occurring in California, it is the adjusted non-orographic amount from the December 1937 storm (88) transposed from Oregon to the northern end of the Central Valley, which controls FAFP there by approximately 20 percent over the September 1959 storm (1006).

At the second refining stage of transposition, the horizontal range set during the first stage is limited by: 1) the specific thermal and moisture inflow characteristics of each storm, 2) a reasonable latitude range over which the absolute vorticity of the flow about the storm would remain virtually unchanged, and 3) the distribution of record-setting storms across California. The way in which such considerations are handled in setting horizontal transposition limits has been widely discussed, most recently in HMR 57, Chapter 7.4.

The limit to vertical transposition of the non-orographic storm mechanism is defined as the elevation at which mixed (liquid and frozen) precipitation in a probable maximum storm begins. Mixed precipitation is generally observed at and below 2° Celsius. The procedure to define this elevation is slightly different than used in HMR 57. An upper air climatology (Crutcher and Meserve 1970) was used to determine an elevation at which the ambient air temperature becomes 2° C. This *climatological* elevation was compared with printed records which showed the level where liquid precipitation became frozen during the given storm. The *climatological* elevation is important because the storm mechanism produces only liquid precipitation below it and mixed (freezing, frozen) states of precipitation above it. Climatological elevation considerations mentioned here apply only to techniques relating to the vertical component of transposition. For transposition purposes, the higher of the two elevations was used. Steps in determining the *climatological* elevation are as follows:

- A. At one or more points taken to represent either the whole or a subregion of the horizontal range of transposition of a storm mechanism, find the mean and standard deviation of the geopotential height and ambient air temperature of the 700-mb surface.
- B. Increase the means of the geopotential height and the temperature, obtained by A, by two standard deviations.

- C. Starting with the (increased) height and (increased) temperature from B, and assuming the atmosphere to be saturated and pseudoadiabatic, increase or decrease the starting temperature until a value of 2° C is achieved. Increase or decrease the height by the amount to achieve the required temperature change. The final height is the required *climatological* elevation. The height and temperature changes were performed here using a USAF Skew T, log P Diagram.

6.5 Controlling Storms

Once all the storms had been analyzed using the above procedures the final adjusted values were transposed to a sufficient number of points so that gradients of non-orographic PMP could be defined for all of California. Table 6.1 shows all of the storms from Chapter 5, Table 5.3 and as mentioned in Chapter 5, Section 5.4, only 9 of these storms provided controlling values of FAFP. Figure 6.2 shows regions where the indicated storm *controlled* the convergence component of PMP. In other words, the storm had a higher value of FAFP than any other storm observed or transposed in the region. A storm could be transposed over a wider range than indicated, but in such extended areas its transposed FAFP value would be exceeded by another storm.

There are two stippled areas, one in the high Sierra, and the other along and leeward of the peaks rimming the southern edge of the Mojave Desert and the western edge of the Imperial Valley. These areas are not *controlled* by any of the storms listed in Table 6.1. Instead they are areas in which FAFP is set through implicit transposition. A portion of the FAFP field in California is shown as Figure 6.3. In this figure, the values of FAFP near the 42nd parallel were constrained to the same values as in HMR 57 in that vicinity.

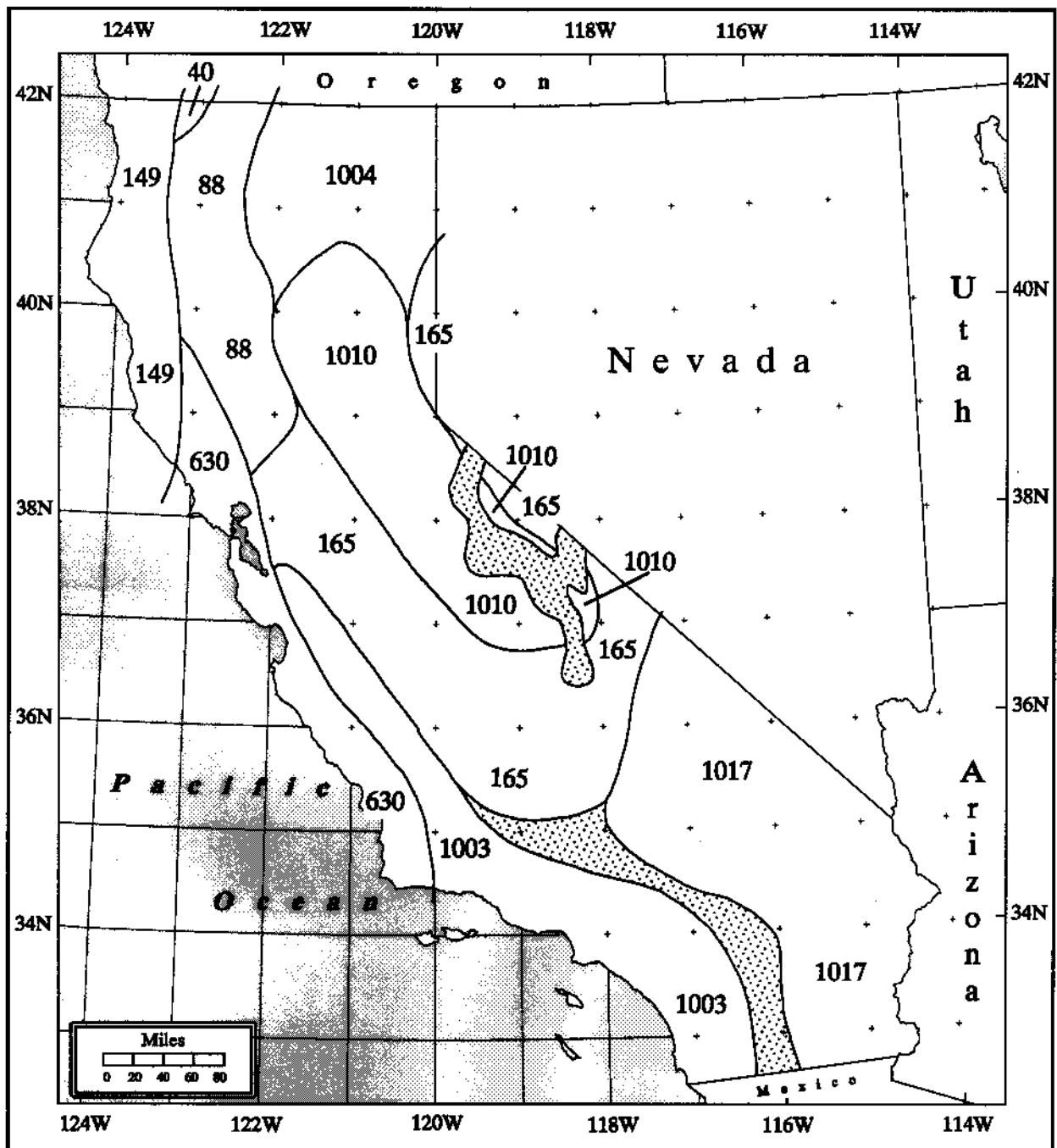


Figure 6.2. *Controlling subregions for 1000-mb, 10-mi², 24-hour maximized convergence storm component (storm identification numbers in Table 6.1). The stippled area represents areas that have FAFP set through implicit transposition.*

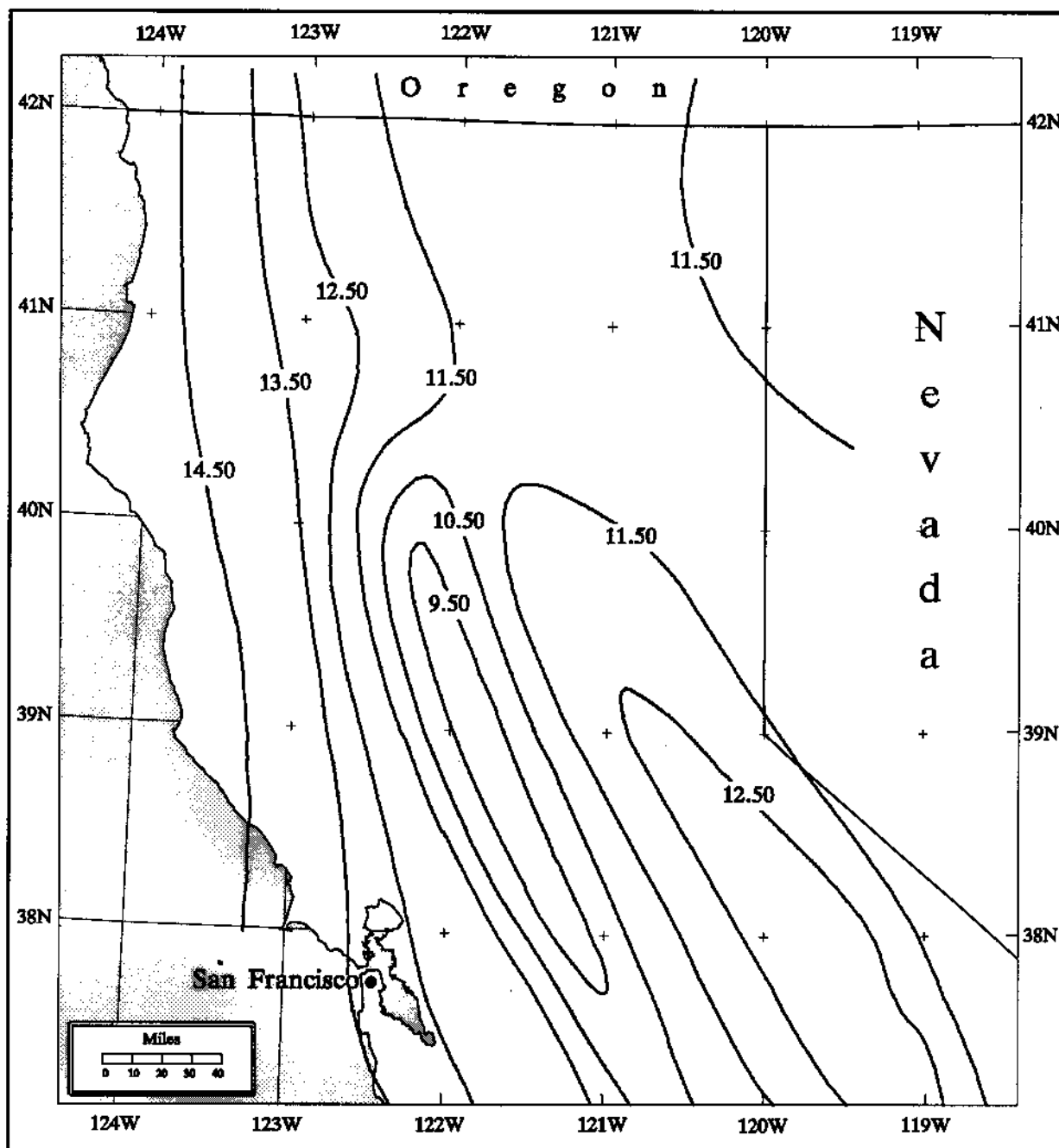


Figure 6.3. *Non-orographic PMP (FAFP) at 1000 mb (inches of rainfall).*

6.6 Determining the Orographic Influence (K) Factor

6.6.1 Introduction

The topographic effect on convergence precipitation, is expressed as a percent increase or decrease of convergence precipitation. Thus:

$$\text{PMP} = K * \text{FAFP} \quad (6-4)$$

where,

K is the orographic factor for the same area and duration, and
FAFP is convergence precipitation for an *index area size* and *index duration*, usually 10-mi² and 24-hour

The K-factor is derived from two relationships: 1) The first involves the one-percent chance (100-year return period) precipitation amount in proximate areas of large and small topographic variation. This relationship is represented by T/C where T is the 100-year, 24-hour return-frequency precipitation; and C is the non-orographic (convergence) component of T. 2) The second concerns the accumulation rate and absolute depth of non-orographic precipitation from record-setting storms. It is represented by M which is the ratio of the precipitation depth of in a *core* period to the depth during the *index duration*. The *core* period is the longest, contiguous of time interval within an *index duration* during which:

- A. The accumulated *core* precipitation equals or exceeds some arbitrarily long return period (usually 100 years), and also
- B. The ratio of the proposed *core* amount (as a percent of the index amount) to the proposed *core* duration (as a percent of the index duration) equals or exceeds 2.

The depths used in A and B above are obtained from the mass curves of precipitation at locations of minimal topographic variation. It is assumed that those precipitation rates are representative of the non-orographic rain rates at the storm center. The K-factor is evaluated from the expression:

$$K = M^2 (1 - (T/C)) + (T/C) \quad (6-5)$$

where,

- K is the orographic factor,
- M is the storm intensification factor,
- T is the 100-year, 24-hour precipitation value, and
- C is the 100-year convergence component.

This expression has been discussed in HMR 55A and other reports (Fenn 1985, Miller et al. 1984, WMO 1986).

6.6.2 Determining the (T/C) Ratio

The denominator (C) of the ratio was determined in two steps:

- A. 100-year, 24-hour values from areas of non-orographic topographic characteristics were adjusted to a 1000-mb reference level using the 12-hour maximum persisting dewpoints from Chapter 4, Figure 4.16, and smooth analysis of these values drawn. The analysis near the 42nd parallel in California was made to match the analysis in Oregon used in HMR 57. The vertical adjustments were based on the barrier elevations (Chapter 3, Figure 3.4) and a 1000-mb persisting dewpoint field, representative of the season in which storms produce precipitation depths near the 100-year level. The analysis was interpolated smoothly from the calculated values unless modification of the field were indicated by climatology or by physiographic features.
- B. The results from Step A are then adjusted from 1000 mb to the barrier elevation using the same persisting dewpoint field as in Step A. The resulting values are the calculated point values for the denominator (C) of the ratio.

Figure 6.4 is the T/C field for California. In some places, the calculated value of T/C was less than one. When physiographic features explained the low values, they were accepted; otherwise, values were set to one.

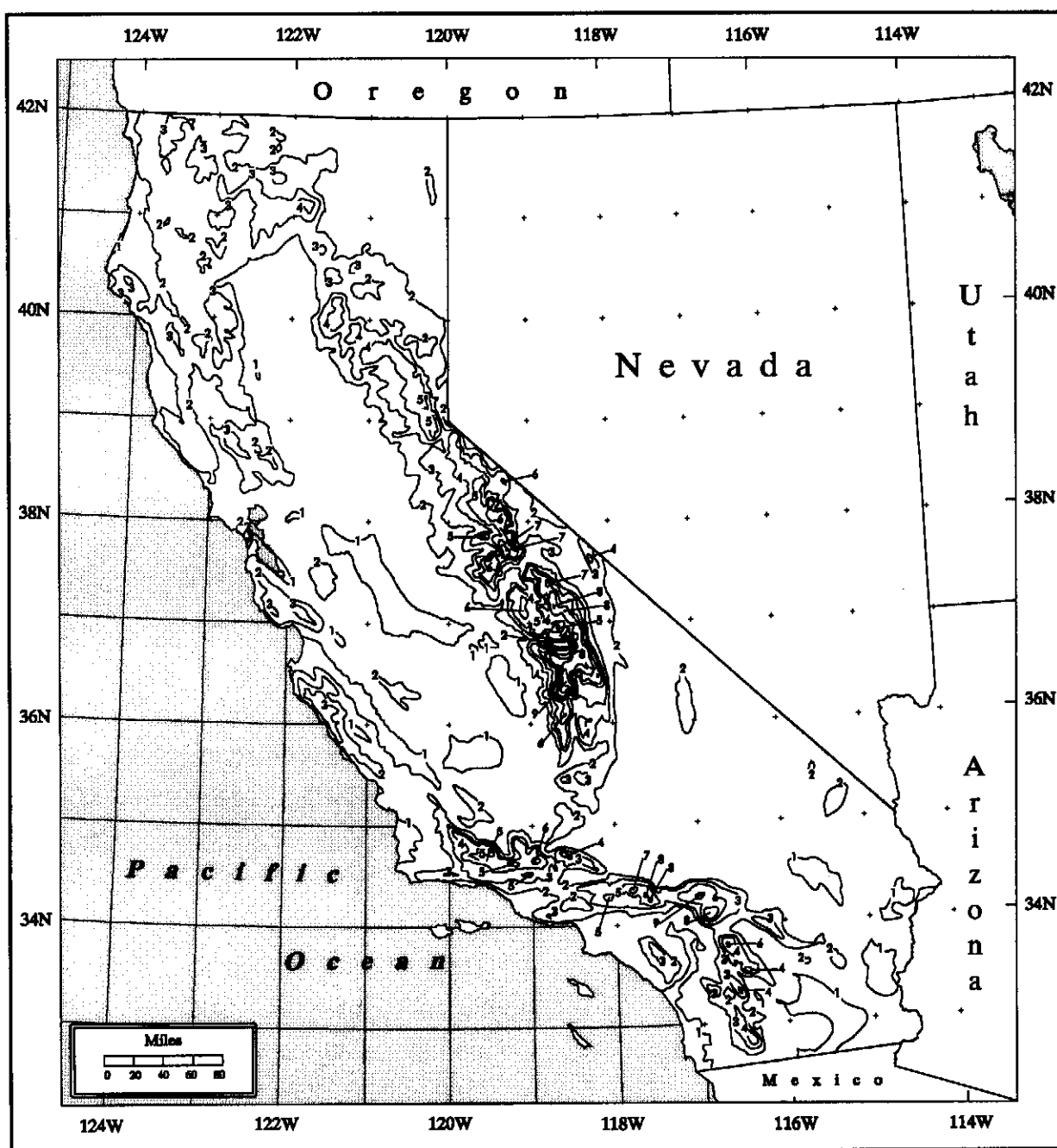


Figure 6.4. Computer produced analysis of the orographic factor, T/C.

In Chapter 7, a number of subjective changes made to preliminary versions of the 10-mi², 24-hour Index map of PMP are discussed. Some of these changes were prompted by examination of the T/C parameter, the principal determinant of the K-factor. In some instances, low NOAA Atlas 2 (1973) 100-year, 24-hour depths were believed to underestimate the orographic potential for enhancement of convergence precipitation. In other instances, it was an overestimate of the convergence component of the 100-year, 24-hour depths, which then caused the underestimation first of T/C, then of the K-factor and finally of index PMP. At other times, unusually high index PMP depths may have resulted from underestimation of the convergence component. A rule was adopted, that when the orographic factor was the causative factor in an untenable estimate of index PMP and where NOAA Atlas 2 100-year, 24-hour depths in an area were valid, changes to the denominator, C, of the T/C ratios were made as long as the changes did not result in anomalous localized values in the analyzed field of C.

6.6.3 Determining the M-factor

Table 6.2 lists the storms controlling the level of FAFP in California, along with the M-factor associated with each of these storms. The storm intensification factor, M, relates the precipitation in the most intense rain period to the total rainfall within the storm period, and therefore varies with storm type. Only two of these storms the February 1986 (1010) and the January 1974 (165) events have intensification factors that are not zero. The M-factor for the January 1974 storm (165) was a compromise value of 0.24. The compromise arose because the M-factor requires that not only the normalized rain rate exceed an acceptable level, but also that the precipitation depth during a *core* period exceed another acceptable level. This storm had a slightly shorter return-period definition for the depth and yielded an intensification factor of 0.38, while strict adherence to a 100-year level definition caused the M-factor to drop to zero. This instance highlights just one of the problems associated with defining a physically meaningful factor by arbitrarily set levels. Somewhat the same situation exists for storm 1003 where both the rain rate and the level of core precipitation are both below the acceptable level. Storm 1010 poses a different problem in that its intensification factor of 0.65 is achieved by having acceptably large values for rain rate and level of core precipitation, but an M-factor this large is more representative of a warm, moist season PMP storm which is not the season for the maximum, all-season storm in the Sierra. It was determined that an M-factor with a lesser, more winter-

like value in the range of 0.30 to 0.40 in the Sierra region would be used for storm 1010. Using a higher value would have resulted in a 29 to 37 percent reduction in total PMP in the more highly orographic sections of the region. Reduction of PMP to this extent was considered untenable.

Table 6.2. <i>Value of storm intensification factor M for storms setting the level of FAFP.</i>		
Storm ID	Date	M-Factor
630	1/3-5/1982	0.0
1003	1/20-24/1943	0.0
1004	11/17-21/1950	0.0
1010	2/14-19/1986	0.65
1017	8/15-17/1977	0.0
Storms used in other HMR studies		
40	12/9-12/1921	0.0
88	12/26-30/1937	0.0
149	11/21-24/1961	0.0
165	1/14-17/1974	0.38

It will be recalled from Section 6.4 that transposed values from the (winter-time) January storm 1937 (88) with an M-factor of zero, set the FAFP level in the northern Central Valley. The September 1959 storm (1006) had a lower transposed value of FAFP and an M-factor of 0.59. However, storm 1006 is considered to be an *off-season* storm and so its M-factor was not weighted as highly as that of the January 1937 storm (88) when setting values in the northern end of the Central Valley. Compromise values between 0.25 and 0.32 are used in this region rather than a value exactly as observed. Thus, the analysis of the storm intensification parameter incorporates considerable modification to the directly calculated M-factors based on the profiles (mass curves) of the largest observed non-orographic precipitation from record-setting storms across the state. Figure 6.5 shows the storm intensity or M-factor analysis. The largest values of the M-factor for all of California approach 0.55 in the extreme southeastern part of the state. Minimum storm-intensity potential (low M-factor) is along the Pacific coastline, with a secondary minimum in a quite narrow zone to the lee of the Sierra crests along the Nevada border. The all-season PMP storm in this secondary area is a winter-time phenomenon, as will be seen in Chapter 7, Figures 7.2 through 7.11.

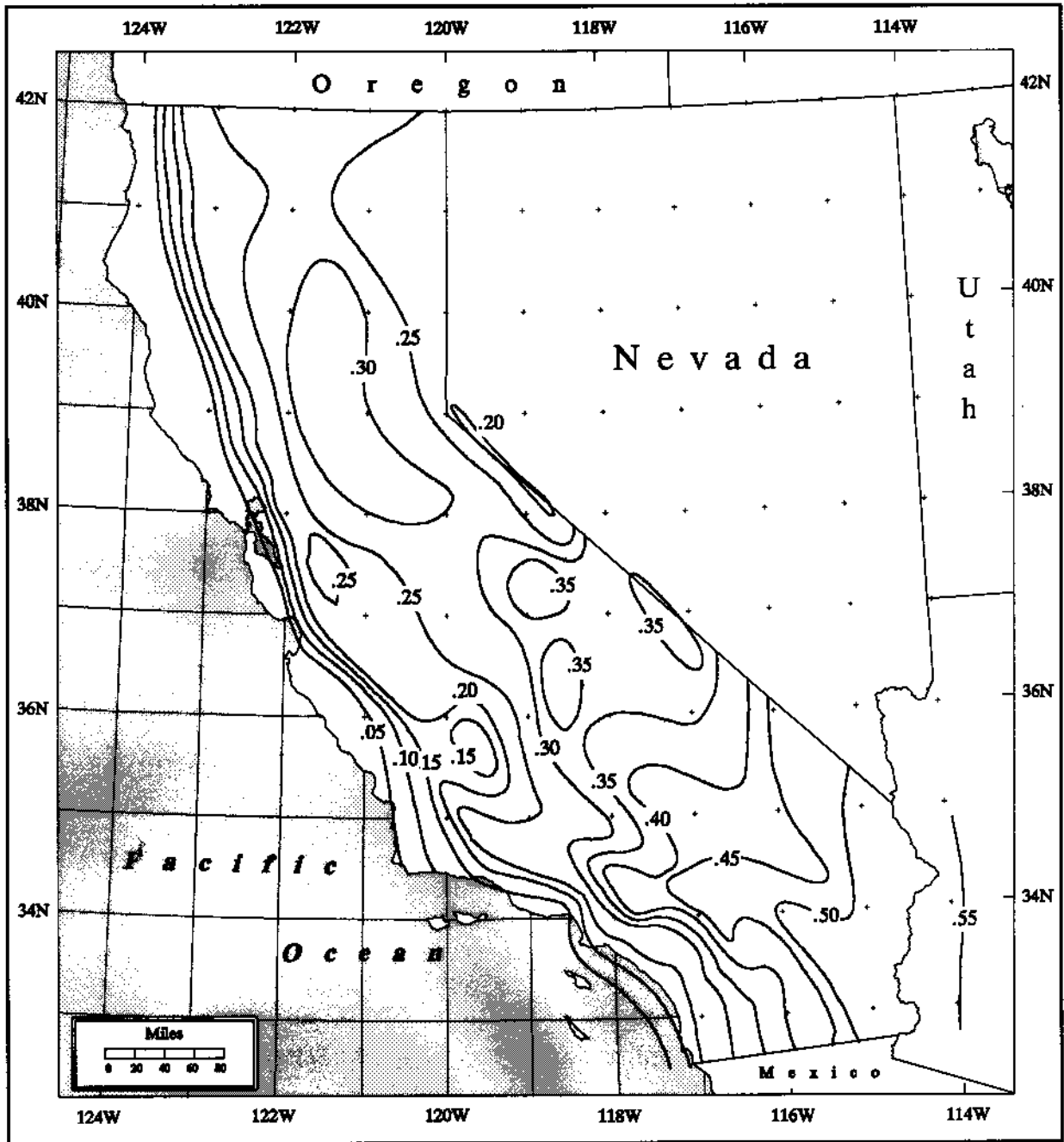


Figure 6.5. Storm intensity (*M*-factor) map.

During peer review concern was expressed that the somewhat subjective modifications made to M-factors, based on meteorological judgement, threatened the credibility of the (orographic) K-factor calculations. Unfortunately, many of the major California storm centers are not found in unambiguously non-orographic areas. The M-factor is a non-orographic storm property which should be determined as close as possible to the storm center. Consequently, varying degrees of uncertainty are associated with M-factors for those storms where the mass curves of rainfall come from non-orographic locations considerably removed from the storm center. In such cases when available mass curves indicate M-factors out-of-line with values found in other storms, meteorological judgement was exercised.

K-factors are not as sensitive to variation in M-factor as they are to variation in T/C, as can be seen in Table 6.3. A three-fold *uncertainty* as to the *correct* T/C produces an approximate 250 to 300 percent change in the resulting K-factor (over the range of M-factors shown), whereas, a three-fold *uncertainty* in the M-factor (over the range of T/C shown) produces only a 20 to 40 percent change in the resulting K-factor. In other words, if we are quite confident in our value for T/C, that should mitigate considerably our uncertainties in the resulting K-factor. But, alas, a variation of *only* 20 percent in a K-factor is not insignificant in absolute terms. We believe that our exercise of meteorological judgement has kept our uncertainties about the K-factors used in this report to a minimum and has produced far better results than would have been the case had we not modified what we believed were unrepresentative M-factors for certain storms.

Table 6.3 <i>Sample K-factors resulting from indicated values of (T/C) and M.</i>				
M	T/C	2.00	3.00	6.00
0		2.00	3.00	6.00
.1		1.99	2.98	5.95
.2		1.96	2.92	5.80
.3		1.91	2.82	5.55
.4		1.84	2.68	5.20
.5		1.75	2.50	4.75
.6		1.64	2.28	4.20